Coherent Exciton-Phonon Coupling in CdSe/ZnS Nanocrystals Studied by Two-Dimensional Electronic Spectroscopy

Rui Wang, Xin-yu Huang, Chun-feng Zhang, Xiao-yong Wang, and Min Xiao

---

Articles you may be interested in

ARTICLE

Coherent Exciton-Phonon Coupling in CdSe/ZnS Nanocrystals Studied by Two-Dimensional Electronic Spectroscopy[†]

Rui Wang[a], Xin-yu Huang[a], Chun-feng Zhang[a*], Xiao-yong Wang[a], Min Xiao[a,b]

a. National Laboratory of Solid State Microstructures, School of Physics, and Collaborative Innovation Center of Advanced Microstructures, Nanjing University, Nanjing 210093, China
b. Department of Physics, University of Arkansas, Fayetteville, Arkansas 72701, USA

Coherent exciton-phonon coupling in CdSe/ZnS nanocrystals have been investigated by temperature-dependent two-dimensional electronic spectroscopy (2DES) measurements. Benefiting from the ability of 2DES to dissect assembles in nanocrystal films, we have clearly identified experimental evidences of coherent coupling between exciton and phonon in CdSe/ZnS nanocrystals. In time domain, 2DES signals of excitonic transitions beat at a frequency resonant to a longitudinal optical phonon mode; in energy domain, phonon side bands are distinct at both Stokes and anti-Stokes sides. When temperature increases, phonon-induced exciton dephasing is observed with dramatic broadening of homogeneous linewidth. The results suggest exciton-phonon coupling is essential in elucidating the quantum dynamics of excitonic transitions in semiconductor nanocrystals.

Key words: Two dimensional spectroscopy, Nanocrystal, Eciton-phonon coupling, Dephasing

I. INTRODUCTION

In the past three decades, semiconductor nanocrystals have attracted tremendous research attention as a model system to understand the physics of exciton confinement [1, 2]. Optical and electronic properties of semiconductor nanocrystals are controllable via the control of size, shape and crystallographic structures, making semiconductor nanocrystals promising for myriad optoelectronic applications including light-emitting diodes [3−5], lasers [6, 7], and photodetectors [8, 9]. In semiconductor nanocrystals, the fundamental properties are highly related to excitonic behavior. Arising from the three-dimensional size confinement, the excitonic transitions exhibit discrete levels. Hence, semiconductor nanocrystals are often quoted as "artificial atoms". The atom-liked quantum behaviors in these nanocrystals also stimulated rapidly-growing interest to explore the possibility of demonstrating solid-state nanocrystal devices for quantum information applications [10, 11]. Towards this end, it is essential to understand the quantum dynamics of excitonic transition in semiconductor nanocrystals.

In the most widely studied system of CdSe nanocrystals, nanocrystals exhibit significant size-dependent properties with sizes comparable to the exciton Bohr radius [12]. In the ensemble level, the size heterogeneity results in a broad inhomogeneous linewidth of the excitonic transition in CdSe nanocrystals [13−15], hindering the probe of intrinsic dephasing process with conventional approaches. To address this issue, photoluminescence spectroscopy measurements have been carried out on single particle level [11, 16, 17]. It has been evidenced that the excitonic transition in single nanocrystals with efficient single-photon emission can be approximately described as quasi-two-level quantum system by properly accounting its coupling to the environment. Despite the fact that many fundamental properties have been uncovered by single-particle spectroscopy, the exciton dynamics, especially in ultrafast time scale (i.e., sub-picosecond), has been challenging due to the limitation of weak signal in individual nanocrystals.

Two-dimensional electronic spectroscopy (2DES) can tackle this challenge with the ability to dissect assembles [13−15, 18−24]. The capability to overcome inhomogeneous broadening makes 2DES ideal to study the quantum dynamics of excitonic transitions in semiconductor nanocrystals. In general, 2DES measures the electric field of a coherently generated four-wave mixing (FWM) response as a function of two time variables: the delay τ between two excitation pulses and the time t over which the FWM signal is emitted [19, 22]. The Fourier transform with respect to the two time variables generates the signal of 2D spectrum as a function of two frequencies, i.e., an excitation frequency (ω_τ) and an emission frequency (ω_t) [24]. The 2D spectrum

---

     637

probes the members of the ensemble in multiple time points, which can principally extract the information of individual nanocrystals [24]. More importantly, the signal of a 2D spectrum accesses not only the populations occupied at each states but also the quantum coherence between these states [25]. The dynamics of population and coherence can be studied by recording 2D spectra as a function of population delay (T) between the second and third pulses, which are informative for describing the quantum dynamics of nanocrystals [14, 15, 20, 22, 26].

In this work, we study the coherent exciton-phonon coupling in CdSe/ZnS nanocrystals by temperature-dependent 2DES measurements. We have observed experimental evidences of coherent exciton-phonon coupling with 2D signal beating at the frequency of LO phonon mode in time domain and phonon side bands in energy domain. When temperature increases, phonon-induced exciton dephasing is clearly observed with dramatic broadening of homogeneous linewidth. The results suggest exciton-phonon coupling plays a key role in determining the quantum dynamics of excitonic transitions and optical properties in semiconductor nanocrystals.

II. EXPERIMENTS

A. Samples

The CdSe/ZnS nanocrystals used in the experiments were obtained commercially. The lowest excitonic transition $|X_1\rangle$ (1S$_{(3/2)}$(h)-1S(e)) is $\sim$2.01 eV at room temperature. We prepared thin-film samples by the spin-coating approach for measurements at cryogenic temperatures. The substrate of a 0.4 mm-thick sapphire plate was chosen to ensure good thermal conduction at low temperatures. The thickness of the film sample was calibrated by the absorption at the lowest excitonic transition. The data reported in this work were recorded from a film sample with optical density of 0.3 at the excitonic resonance.

B. 2DES measurements

We utilized a broadband 2DES setup developed in our group recently [27]. Breifly, the setup is configured in a pump-probe geometry with active phase locking approach as described previously (FIG. 1(a)) [27]. Two home-built nonlinear optical parametric amplifiers (NOPAs) pumped by a 1 kHz commercial regeneration amplifier (Libra, Coherent) at 800 nm were used as the light sources. The output beams with tunable spectral coverage were compressed by a pair of chirped mirrors and a quartz wedge pair to near transform limit with temporal pulse duration of $\sim$7 fs. The output from one NOPA was employed to gen-
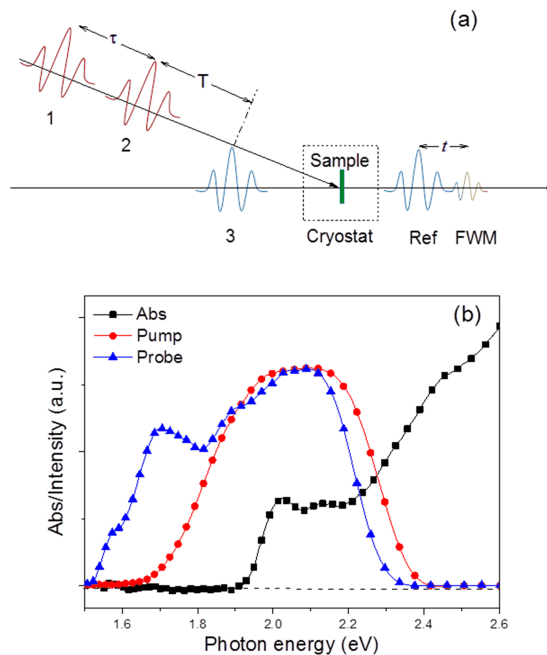

FIG. 1 (a) Schematic diagram of broadband 2DES setup configured in pump-probe geometry. (b) Spectra of pump (pulse 1 & 2) and probe (3 & Ref.) beams are shown in comparison with the absorption spectrum of CdSe/CdS nanocrystals at room temperature.

erate the two phase-locked collinear excitation pulses (1&2, FIG. 1(a)) with desired temporal delay τ. The phase stabilization was achieved with the interferogram signal of a co-propagated cw beam in Mach-Zehnder interferometer by active feedback electronics [28]. The output from the other NOPA was adopted as the third probe pulse (3, FIG. 1(a)), which is also employed as the reference beam (Ref., FIG. 1(a)), *i.e*, the local oscillator for heterodyne detection of FWM signal. The interferogram between the signal and the local oscillator was analyzed by a silicon CCD (S11071, Hamamatsu) coupled to a monochromater in a pulse-to-pulse mode enabled by a custom-designed control board from Entwicklungsbuero Stresing. The spectral resolution is $\sim$7 meV with a 300 g/mm grating for covering the whole probe wavelength range.

To obtain the population dynamics, we scanned population time T up to 400 ps. The samples were mounted in a cryostat (MicroHe, Oxford) for temperature-dependent experiments. The spectra of pump and probe beams were set to cover the two absorption peaks of the CdSe/ZnS nanocrystals (FIG. 1(b)). The pump fluence at the sample was kept to below 20 μJ/cm^2 to minimize the effect of exciton-exciton interaction. The overall temporal resolution of our setup is better than 10 fs in population decay. We checked the polarization dependence and found the major feature of absorptive 2D spectrum of CdSe/ZnS is insensitive to the polarization configuration. The data shown in this work
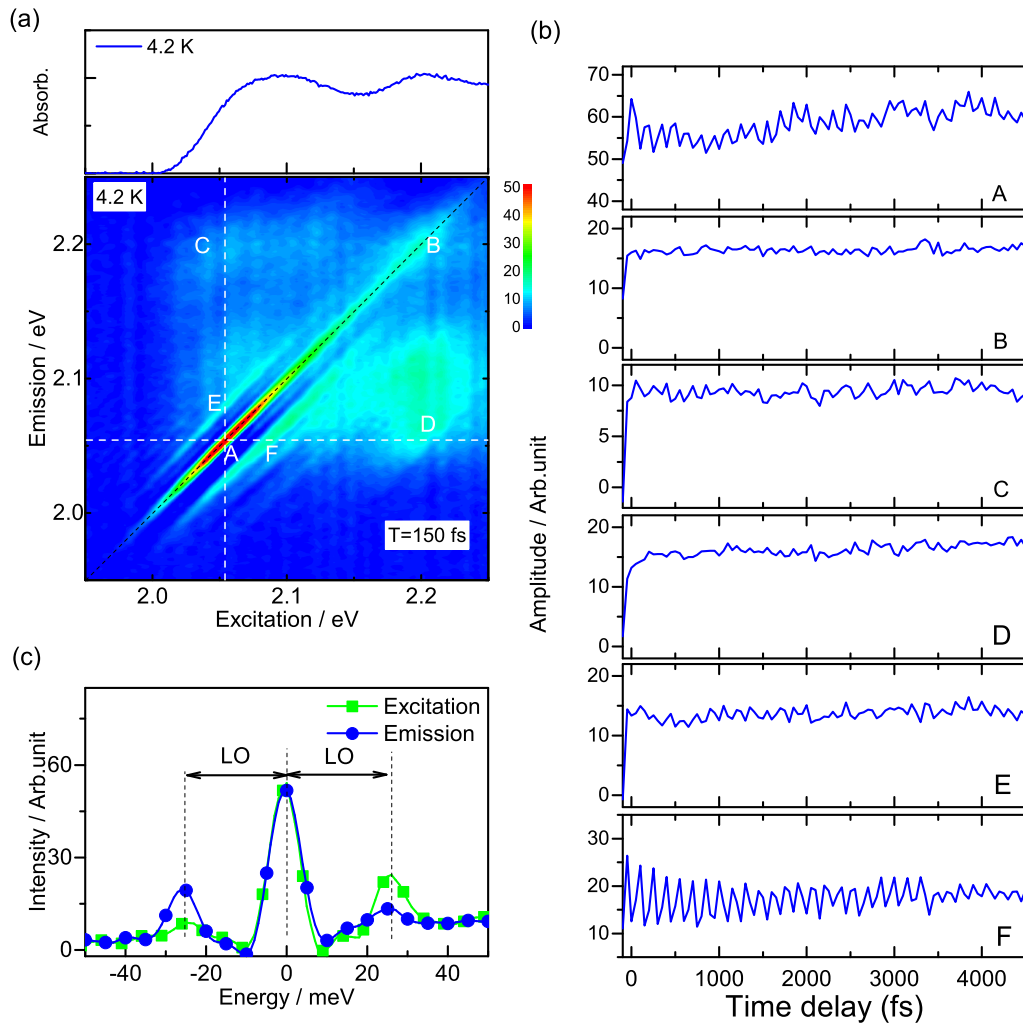
FIG. 2 (a) Absorptive 2D spectrum recorded from the film sample of CdSe/ZnS nanocrystals is shown in comparasion with the 1D absorption spectrum. The data were recorded at 4.2 K with population delay T=150 fs. (b) Temporal evolution dynamics of 2DES signals recorded at different excitation/emission energies marked as A−F in (a). (c) The slice spectra marked as the white dashed lines in (a) show the excitation spectrum and the emission spectrum resonant to the lowest excitonic transition.

were recorded with the cross polarized pump and probe beams.

III. RESULTS AND DISCUSSION

FIG. 2 shows the results of a 2DES measurement on CdSe/ZnS nanocrystals at 4.2 K. The absorptive 2D spectrum (FIG. 2(a)) recorded at a population decay T=150 fs shows the resonant transition energy of the $|X_1\rangle$ exciton is 2.06 eV, which is slightly blue shift with respect to that at room temperature (FIG. 1(b)). The second excitonic transition peak $|X_2\rangle$ appears at 2.20 eV, which has been frequently assigned to a higher excitonic transition $(2S_{(3/2)}(h)\text{-}1S(e))$ [29]. We plot the dynamics of the diagonal and anti-diagonal signals resonant to $|X_1\rangle$ and $|X_2\rangle$ transitions marked at A, B, C, & D in FIG. 1(a). The simultaneous buildup of the signal

at C suggests the coherent electronic coupling between the $|X_1\rangle$ and $|X_2\rangle$ transitions, which is reasonable since the two excitonic transitions share the same excited levels (1S(e)).

The dynamic of peak A clearly shows a slow decay at late stage and a rapid oscillation in the first 5 ps. The slow decay component is related to the exciton recombination in CdSe/ZnS nanocrystals, which is in a timescale of nanoseconds and beyond the delay range in this experiment. The fast oscillation frequency is estimated to be $\sim$218 cm^{-1}, which is close to a longitudinal optical (LO) phonon mode in CdSe/ZnS nanocrystals [14, 30], implying the coherent exciton-phonon coupling is a possible reason for the oscillatory behavior. This assignment is further confirmed by observation of two sidebands in the 2D spectrum with energy below and above the major excitonic feature A, respectively
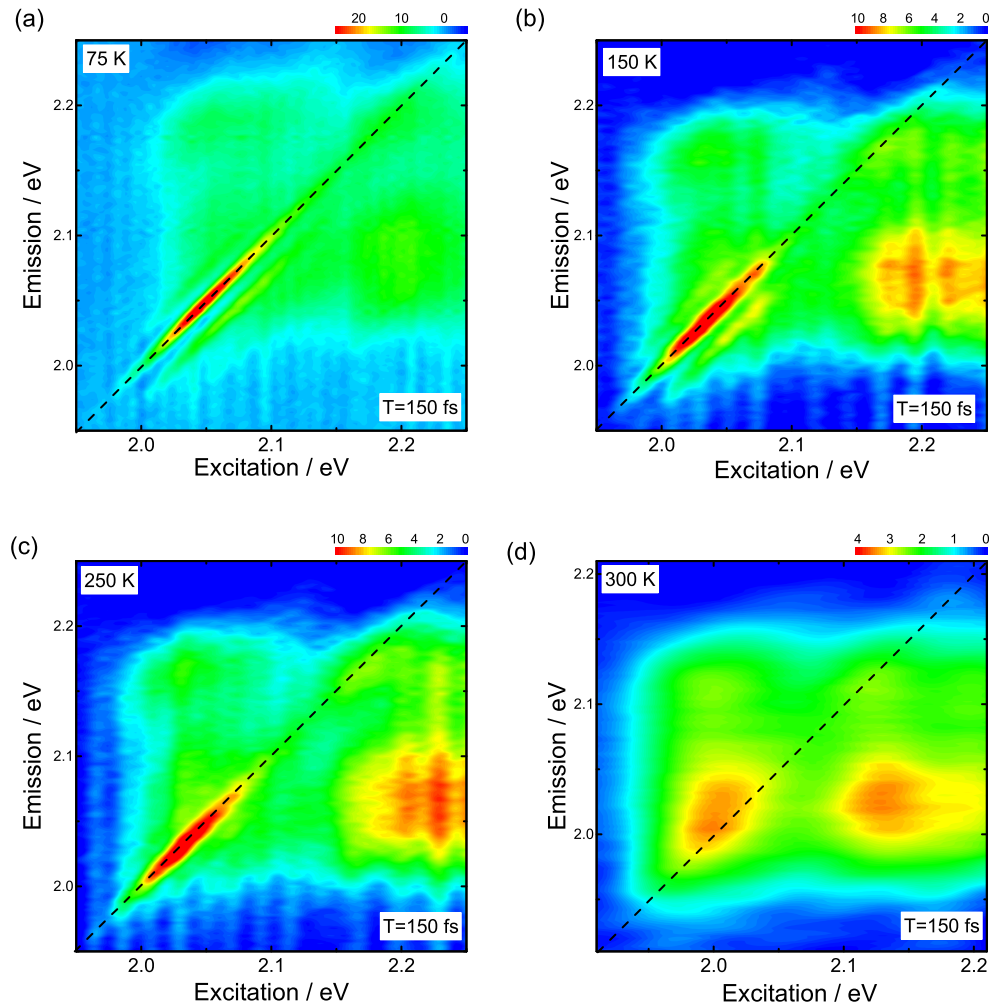

FIG. 3 Absorptive 2D spectra of the film sample of CdSe/ZnS nanocrystals recorded at different temperatures. The population time T=150 fs.

(FIG. 2(a)). We plot in FIG. 2(c) the spectra of vertical and horizontal slices in the 2D spectrum to show the fine features of the emission and excitation spectra. The two side peaks are the same energy and different from the major peak A in both emission and excitation spectra. The energy shift is ∼26.5 meV, agreeing well with the oscillation frequency (∼218 cm^{-1}). Moreover, the 2D signals probed on the sideband peaks (E & F, FIG. 2(b)) show oscillations at the same frequencies. These coincidences clearly indicate the observed result is tightly related to the coherent coupling between exciton and LO phonon mode. The two side peaks can be assigned to the phonon sidebands (*i.e.*, $|X_1\rangle$+LO, and $|X_1\rangle$-LO states). These fine structures cannot be distinguished in 1D absorption/emission spectra due to the broad inhomogeneous linewidth since 1D absorption/emission spectrum is a projection of 2D spectrum in the frequency domain of excitation/emission, respectively [12].

Next, we try to understand the effect of exciton-phonon coupling on the quantum dephasing dynamics of excitons. On this issue, 2D spectrum is much more informative than conventional 1D spectrum. The signal is narrowly distributed anti-diagonally but broadly distributed diagonally, representing the homogeneous and inhomogeneous linewidths of the measured system [31]. In the impulsive pulse approximation, the homogeneous linewidth is proportional to the full-width at half maximum (FWHM) of anti-diagonal profile (*i.e.* $\gamma \propto$ FWHM/$2\sqrt{2}$) [32, 33]. The homogeneous linewidth directly reflects the dephasing process of excitonic transitions in CdSe/ZnS nanocrystals, which describes the difference between the excitonic transition and an ideal two-level quantum system. The presence of phonons due to lattice vibration is one major difference between the two-level systems in atoms and semiconductor nanocrystals, which is likely to be the major difference in the resonance broadening mechanism. We study the dephasing induced by the exciton-phonon coupling by performing the temperature-dependent 2DES measurements. In FIG. 3, we show the 2D spectra of the same sample at different temperatures, respec-
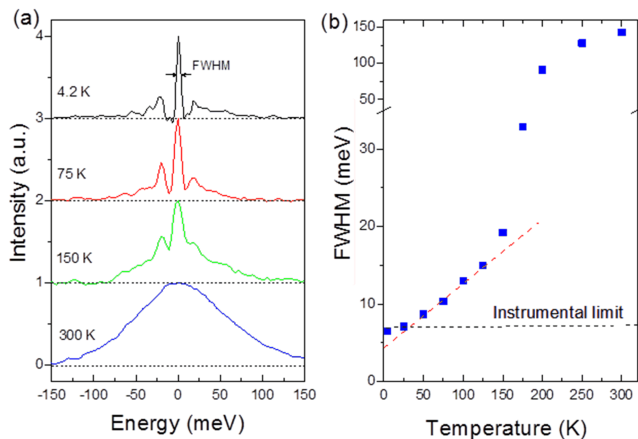
FIG. 4 (a) Anti-diagonal profiles probed with energy resonant the lowest excitonic transitions at different temperatures. The FWHM linewidth (b) of anti-diagonal profile is plotted versus temperature. At relatively low temperature (<100 K), the linewidth is linearly dependent on temperature as a consequence of single-phonon scattering.
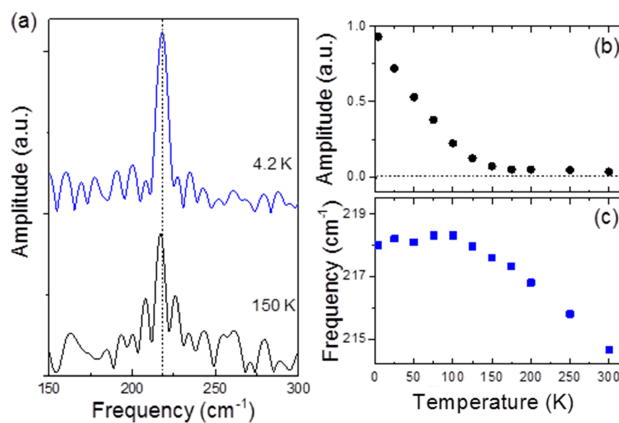

FIG. 5 (a) Fourier transform spectra of the LO phonons derived from the beating signal in 2D spectra recorded at 4.2 and 150 K, respectively. The amplitude (b) and frequency (c) of the beating signal are plotted versus temperature, respectively.

tively. When temperature increases, the linewidth of anti-diagonal profile becomes broader as a clear signature of photon-induced dephasing of excitonic transition. At higher temperatures, the phonon sidebands are mixed with the resonance $|X_1\rangle$ signal as shown in the anti-diagonal profiles recorded at different temperatures (FIG. 4(a)), which is probably the reason why the phonon sidebands have never been reported in previous 2DES measurements on CdSe/ZnS nanocrystals [14, 15, 19].

To quantify the role of phonons, we plot FWHMs of the anti-diagonal profile as a function of temperature in FIG. 4(b). The FWHM increases from ∼7 meV at 4.2 K (limited by the instrumental limit) to ∼143 meV at 300 K, clearly indicating the increasing of homogeneous linewidths when more phonons are activated with increasing temperature. Notably, in the low temperature range (<100 K), the linewidth is linear dependent on the temperature. By assuming the major dephasing mechanism to be the scattering with acoustic phonons, such behavior can be understood within a single-phonon scattering model [34]. In this scenario, the temperature dependent linewidth can be expressed as $\gamma(T)=\gamma(0)+\gamma'T$, where $\gamma(T)\propto$FWHM$(T)/2\sqrt{2}$ is the linewidth at temperature T, $\gamma(0)$ represents the residual line width at zero temperature and γ' denotes the electron-phonon coupling strength. Fitting to the experimental data (red line in FIG. 4(b)) in the temperature range <100 K, the values of $\gamma(0)$ and γ' can be roughly estimated to be ∼1 meV and ∼36 μeV/K, respectively. These values are comparable to the typical values in semiconductors like GaAs and transition metal dichalcogenides [31, 35, 36].

Coherence of lattice vibration in the CdSe/ZnS nanocrystals at room temperature has been widely studied by several groups using 2D spectra and pump-probe techniques [12−15, 18, 23, 25]. It has been demonstrated that the size of the nanocrystals and the type of the ligands may affect the vibrational coherence in this system [12, 14], while the effect of temperature has been rarely explored. We focus on studying the temperature-dependent beating behavior related to LO phonon mode to study coherent lattice vibration in this system (FIG. 5(a)). The decoherence process is directly reflected by the linewidth of LO mode of ∼218 cm^{-1}. The FWHM of the peak of LO mode at 218 cm^{-1} remains to be nearly independent of temperature with a value of ∼8.7 cm^{-1} which is comparable with the value measured by another approach [12]. These results suggest that the decoherence process of lattice vibration is insensitive to temperature in CdSe/ZnS nanocrystals. Nevertheless, the amplitudes of the oscillatory component decrease dramatically at higher temperatures, which may be caused by the fast electronic dephasing at room temperature. In addition, the frequency of the LO phonon mode in the CdSe/ZnS nanocrystals decreases dramatically when temperature increases, which is comparable with the temperature-dependent Raman scattering measurements in many solids [37, 38].

IV. CONCLUSION

In this work, we have performed temperature-dependent 2DES measurements to study coherent behavior of exciton-phonon coupling in CdSe/ZnS nanocrystals. The coherent coupling between exciton and phonon is manifested with 2D signal beating at the frequency of LO phonon mode in time domain and phonon sidebands in energy domain. When temperature increases, the decoherence of lattice vibration

is likely to be independent of temperature; However, the homogeneous linewidth of excitonic transition becomes broader due to phonon-induced exciton dephasing. The results suggest exciton-phonon coupling is essential in determining the quantum dynamics and optical responses of excitonic transitions in semiconductor nanocrystals.

V. ACKNOWLEDGMENTS

[1] V. I. Klimov, *Nanocrystal Semiconductor Nanocrystals*, Boca Raton: CRC Press, (2010).

[2] A. P. Alivisatos, Science **271**, 933 (1996).

[3] N. Tessler, V. Medvedev, M. Kazes, S. H. Kan, and U. Banin, Science **295**, 1506 (2002).

[4] V. L. Colvin, M. C. Schlamp, and A. P. Alivisatos, Nature **370**, 354 (1994).

[5] X. Dai, Z. Zhang, Y. Jin, Y. Niu, H. Cao, X. Liang, L. Chen, J. Wang, and X. Peng, Nature **515**, 96 (2014).

[6] F. Fan, O. Voznyy, R. P. Sabatini, K. T. Bicanic, M. M. Adachi, J. R. McBride, K. R. Reid, Y. S. Park, X. Li, A. Jain, R. Quintero-Bermudez, M. Saravanapavanantham, M. Liu, M. Korkusinski, P. Hawrylak, V. I. Klimov, S. J. Rosenthal, S. Hoogland, and E. H. Sargent, Nature **544**, 75 (2017).

[7] V. I. Klimov, S. A. Ivanov, J. Nanda, M. Achermann, I. Bezel, J. A. McGuire, and A. Piryatinski, Nature **447**, 441 (2007).

[8] G. Konstantatos and E. H. Sargent, Nature Nanotechnol. **5**, 391 (2010).

[9] V. Sukhovatkin, S. Hinds, L. Brzozowski, and E. H. Sargent, Science **324**, 1542 (2009).

[10] N. Somaschi, V. Giesz, L. De Santis, J. C. Loredo, M. P. Almeida, G. Hornecker, S. L. Portalupi, T. Grange, C. Antón, J. Demory, C. Gómez, I. Sagnes, N. D. Lanzillotti-Kimura, A. Lemaítre, A. Auffeves, A. G. White, L. Lanco, and P. Senellart, Nature Photon. **10**, 340 (2016).

[11] P. Michler, A. Imamoglu, M. D. Mason, P. J. Carson, G. F. Strouse, and S. K. Buratto, Nature **406**, 968 (2000).

[12] C. Lin, K. Gong, D. F. Kelley, and A. M. Kelley, J. Phys. Chem. C **119**, 7491 (2015).

[13] S. Dong, D. Trivedi, S. Chakrabortty, T. Kobayashi, Y. Chan, O. V. Prezhdo, and Z. H. Loh, Nano Lett. **15**, 6875 (2015).

[14] T. A. Gellen, J. Lem, and D. B. Turner, Nano Lett. **17**, 2809 (2017).

[15] G. B. Griffin, S. Ithurria, D. S. Dolzhnikov, A. Linkin, D. V. Talapin, and G. S. Engel, J. Chem. Phys. **138**, 014705 (2013).

[16] B. Mahler, P. Spinicelli, S. Buil, X. Quelin, J. P. Hermier, and B. Dubertret, Nature Mater. **7**, 659 (2008).

[17] Y. Chen, J. Vela, H. Htoon, J. L. Casson, D. J. Werder, D. A. Bussian, V. I. Klimov, and J. A. Hollingsworth, J. Am. Chem. Soc. **130**, 5026 (2007).

[18] J. R. Caram, H. Zheng, P. D. Dahlberg, B. S. Rolczynski, G. B. Griffin, A. F. Fidler, D. S. Dolzhnikov, D. V. Talapin, and G. S. Engel, J Phys. Chem. Lett. **5**, 196 (2014).

[19] E. Cassette, J. C. Dean, and G. D. Scholes, Small **12**, 2234 (2016).

[20] F. V. de A. Camargo, L. Grimmelsmann, H. L. Anderson, S. R. Meech, and I. A. Heisler, Phys. Rev. Lett. **118**, 033001 (2017).

[21] E. Harel, S. M. Rupich, R. D. Schaller, D. V. Talapin, and G. S. Engel, Phys. Rev. B **86**, 075412 (2012).

[22] E. Cassette, R. D. Pensack, B. Mahler, and G. D. Scholes, Nature Commun. **6**, 6086 (2015).

[23] N. Lenngren, M. A. Abdellah, K. Zheng, M. J. Al-Marri, D. Zigmantas, K. Zidek, and T. Pullerits, Phys. Chem. Chem. Phys. **18**, 26199 (2016).

[24] S. T. Cundiff and S. Mukamel, Phys. Today **66**, 44 (2013).

[25] S. Pal, P. Nijjar, T. Frauenheim, and O. V. Prezhdo, Nano Lett. **17**, 2389 (2017).

[26] B. Sun, D. B. Almeida, R. Singh, G. M. Diederich, M. E. Siemens, L. A. Padilha, W. K. Bae, J. M. Pietryga, V. I. Klimov, and S. T. Cundiff, *in 2015 Conference on Lasers and Electro-Optics* (2015).

[27] W. Zhu, R. Wang, C. Zhang, G. Wang, Y. Liu, W. Zhao, X. Dai, X. Wang, G. Cerullo, S. Cundiff, and M. Xiao, Opt. Express **25**, 21115 (2017).

[28] A. D. Bristow, D. Karaiskaj, X. Dai, T. Zhang, C. Carlsson, K. R. Hagen, R. Jimenez, and S. T. Cundiff, Rev. Sci. Instr. **80**, 073108 (2009).

[29] V. I. Klimov, Ann. Rev. Phys. Chem. **58**, 635 (2007).

[30] D. M. Sagar, R. R. Cooney, S. L. Sewall, E. A. Dias, M. M. Barsan, I. S. Butler, and P. Kambhampati, Phys. Rev. B **77**, 235321 (2008).

[31] G. Moody, C. Kavir Dass, K. Hao, C. H. Chen, L. J. Li, A. Singh, K. Tran, G. Clark, X. Xu, G. Berghauser, E. Malic, A. Knorr, and X. Li, Nature Commun. **6**, 8315 (2015).

[32] M. E. Siemens, G. Moody, H. Li, A. D. Bristow, and S. T. Cundiff, Opt. Express **18**, 17699 (2010).

[33] J. D. Bell, R. Conrad, and M. E. Siemens, Opt. Lett. **40**, 1157 (2015).

[34] L. Schultheis, A. Honold, J. Kuhl, K. Köhler, and C. W. Tu, Phys. Rev. B **34**, 9027 (1986).

[35] A. Honold, L. Schultheis, J. Kuhl, and C. W. Tu, Phys. Rev. B **40**, 6442 (1989).

[36] H. P. Wagner, A. Schätz, and R. Maier, Phys. Rev. B **56**, 12581 (1997).

[37] I. Calizo, A. A. Balandin, W. Bao, F. Miao, and C. N. Lau, Nano Lett. **7**, 2645 (2007).

[38] S. Sahoo, A. P. S. Gaur, M. Ahmadi, M. J. F. Guinel, and R. S. Katiyar, J. Phys. Chem. C **117**, 9042 (2013).